2012•2013

FACULTEIT GENEESKUNDE EN LEVENSWETENSCHAPPEN

master in de biomedische wetenschappen: bio-elektronica en nanotechnologie

Masterproef

Optimization of thermal resistance system for biosensors

Promotor :
Prof. dr. Patrick WAGNER

Ahmad Abu Zer

Masterproef voorgedragen tot het bekomen van de graad van master in de biomedische wetenschappen , afstudeerrichting bio-elektronica en nanotechnologie

2012•2013
FACULTEIT GENEESKUNDE EN LEVENSWETENSCHAPPEN
master in de biomedische wetenschappen: bio-elektronica en nanotechnologie

Masterproef

Optimization of thermal resistance system for biosensors

Promotor :
Prof. dr. Patrick WAGNER

Ahmad Abu Zer
Masterproef voorgedragen tot het bekomen van de graad van master in de biomedische wetenschappen , afstudeerrichting bio-elektronica en nanotechnologie

universiteit hasselt | Maastricht University

Preface

This thesis is made as a completion of a two years Master programme in Bioelectronics and Nanotechnology at Hasselt University. Moreover, it is also a conclusion of my senior practical training at the Institute for Materials Research (IMO).

Foremost, I would like to thank the Institute for Materials Research (IMO) for giving me the chance to do my senior practical training. Special thanks to my promoter Prof. Dr. Patrick Wagner for introducing me to the topic and his continuous support. Thanks are extended to Jeroen Broeders and Dieter Croux for the constant supervision as well as for providing necessary information regarding the project. Furthermore I like to thank Prof. Dr. Luc Michiels and Dr. Veronique Vermeeren for their valuable time and input.

Also, I would like to thank Mohammed S. Murib for preparing the DNA samples and Kasper Eersels for preparing the surface-imprinted samples. My gratitude also goes to Stijn Duchateau for his comments and advices.

Last but not least, my family has played an integral role in my graduate studies and so I would like to thank them for their support and unconditional love.

Contents

List of Abbreviation

The following table describes the various abbreviations used throughout the thesis.

Abbreviation	Meaning
CVD	Chemical vapour deposition
D	A derivative term
DC	Direct current
DGGE	Denaturing gradient gel electrophoresis
ds	Double-stranded
EDC	1-ethyl-3-(3-dimethylaminopropyl)carbodiimide
I	An integral term
LAN	Local area network
MPECVD	Microwave plasma-enhanced chemical vapour deposition
NCD	Nano-crystalline diamond
NCM	Non-contact mode
P	A proportional term
PBMC	Peripheral blood mononuclear cells
PBS	Phosphate-buffered saline
PCR	Polymerase chain reaction
PDMS	Polydimethylsiloxane
PID	Proportional-Integral-Derivative
PWM	Pulse-width modulation
QCM	Quartz-crystal microbalances
RPMI	Roswell Park Memorial Institute medium
Rth	Thermal resistance
SCD	Sickle cell disease
SDS	Sodium dodecyl sulfate
SIP	Surface-imprinted polyurethane
SNP	Single nucleotide polymorphism
ss	Single-stranded
SSC	Sodium chloride/sodium citrate
TCu	Copper temperature
THF	Tetrahydrofuran
TL	Liquid temperature
Tset	Set point temperature
UV	Ultraviolet
WIFI	Wireless network

Abstract

One of the most important challenges in the area of genome research is to detect single-nucleotide polymorphism (SNP) mismatches. SNP's are involved in a lot of genetic disorders such as Alzheimer or colon cancer. Mutation analysis to detect SNP's can be done using different techniques based on DNA denaturation process. One of these techniques is Real-time PCR with associated melting curve analysis and denaturing gradient gel electrophoresis (DGGE). However, real-time PCR requires expensive instrumentation and DGGE does not provide information on DNA denaturation kinetics. Hence, a fast, hand-held and low-cost device based on the open source Arduino platform will be used to detect DNA denaturation based on the difference in thermal resistance of double-stranded (ds) and single-stranded (ss) DNA samples. This has been developed recently for SNP's detection based on measuring the thermal resistance (Rth) of the hybridized DNA strands [7].

Optimization of the thermal-sensor device has been done by reducing the overshoot in temperature in order to perform Rth measurements on living cells. The overshoot is reduced by adjusting the PID controller parameters.

In Rth measurements on living cells, the surface-imprinted polyurethane (SIP) layer was imprinted on top of aluminum substrate and target cells were added to be bound on the SIP-binding cavities.

In the last stage, the thermal-sensor device is used to perform thermal experiments on two different types of macrophages: rat alveolar macrophages (cell line NR8383) and mouse leukemic monocyte macrophages (cell line RAW 264.7), as the shape and membrane groups of macrophages can be related to cardiovascular diseases. For example, macrophages in atherosclerosis patients show different antigens on their membranes comparing to macrophages of healthy individuals.

From the living cells thermal measurements, the Rth has increased due to binding of target cells to the binding cavities of the SIP-imprinted on aluminum substrate. This can be used as a detection tool for many diseases such as cancer and cardiovascular diseases.

1. Introduction

The importance of studying DNA denaturation is that it can be used to identify single-nucleotide polymorphism (SNP) mismatches between double strands of DNA. Which is one of the most important challenges in genome research. SNP's are involved in a lot of genetic disorders such as Alzheimer or colon cancer [1, 2].

DNA mismatches can be detected using hybridization-based assays such as micro-arrays assay, which play a main role to allow for an extremely parallelized readout on small sample volumes [3]. Major drawbacks are the need for fluorescent labelling of the target DNA, long reaction times, and the absence of dynamic information on DNA binding kinetics. Alternatively, mutation analysis can be done using different techniques that are based on a denaturation process of the double-stranded (ds) DNA such as real-time polymerase chain reactions (PCR). Real-time PCR with associated melting curve analysis and denaturing gradient gel electrophoresis (DGGE) has become widely used to detect SNPs. Based on the fact that DNA samples containing a SNP are less stable than the perfectly matched DNA samples, resulting in lower melting temperatures comparing to the perfectly matched DNA samples. However real-time PCR requires expensive instrumentation and DGGE is less appropriate for parallelized analysis and does not provide information on DNA denaturation kinetics [4, 5].

To conquer these limitations, numerous label-free detection methods based on electronic readout principles have been proposed in recent literature. One of these methods is DNA denaturation detection by measuring the thermal resistance (Rth) of the hybridized DNA strands, the denaturation detection is based on the difference in thermal resistance of (ds) and single-stranded (ss) DNA samples [5]. The (ds) DNA samples are immobilized on a heat conducting substrate. The temperature of the substrate is controlled by using Proportional-Integral-Derivative (PID) control system. The difference between substrate and liquid temperature can be measured and used to determine the thermal resistance of the DNA samples in respect to the input power of the PID control. The PID control system will increase the substrate temperature and lead to DNA denaturation that causes a sudden shift in the thermal resistivity of the DNA sample. Increasing temperatures will lead to denaturation by breaking the hydrogen bonds of the double stranded DNA , this allows not only for understanding the DNA denaturation kinetics but also to detect SNP's since the denaturation of DNA containing mismatches occurs faster than the denaturation of perfectly matched DNA.

The DNA sample consists of a silicon die covered with a nano-crystalline diamond (NCD) layer. The diamond layer serves as a platform on which the DNA sample will be immobilized on top of the NCD layer. The advantages of using diamond refer to the outstanding thermal, chemical and electrochemical stability and high thermal conductivity that make it very attractive for biochemical and biosensors applications [6].

The liquid cell that contains the DNA samples is connected to a hand-held device, which can be controlled using local area (LAN) or wireless (WIFI) network; this allows automation of the thermal resistance measurements [7].

The PID controller is implemented in the hand-held device and serves as a heating source by applying input power to the resistor placed on the copper contact. PID controllers are the most simple and effective controllers that are used to manipulate processes. The controller allow for much better adjustments to be made in the system by giving the designer large number of options for changing the dynamics of the system.

The PID controller will calculate the difference between the measured process and the desired set point to correct the error between both processes, and then performing an action to adjust the process accordingly. The PID controllers are feedback systems as shown in figure 1, widely used in many control systems and include three parameters:

- A proportional term (P)
- An integral (I)
- A derivative (D)

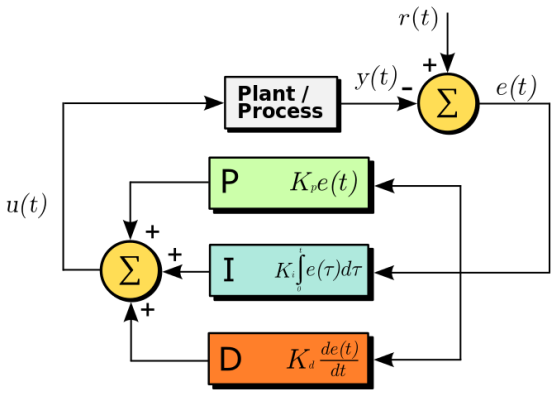

Figure 1: Diagram of a PID controller in a feedback orientation [10]

The proportional (P) action is directly proportional to the control error. The higher the "P" parameter, the faster the system will reach the set-point, but also high proportional gain turns the system unstable and it oscillates around the set-point. On the other hand, if the P is low, then the system will become stable with a constant error above or below the set-point, because the output will not deliver enough power for the system to reach the final position [26,11].

A proportional system is usually not sufficient to remove the error. The system should not only change its output according to the current error, but it should also be able to watch and change the output according to the past errors. **The integral (I) action** is the sum of the errors over time. If the error is large, then the integral builds up as time passes and the output changes quickly to remove the error [26].

The Derivative (D) term determines the rate of change of the error and adds to the output accordingly. If the error changes slowly, then the derivative term should be increased in order to make the system respond faster [11, 26]

Those three parameters are adjustable and controller tuning involves setting these parameters at values which suits the process to be controlled.

DNA denaturation process can be done by applying temperature ramping profile to heat the samples and the set point temperatures (Tset) were set between 25° up to 80°. The PID parameters were set as follows (P=0.8, I=50, D=0); these values are appropriate for applying ramping profiles since the copper temperature (TCu) corresponds nicely to the set point with very small difference in temperature between the copper and the set point. However, when applying constant temperature profile using these parameters (P = 0.8, I = 50, D = 0), a high overshoot in (TCu) appears. For example, the overshoot in (TCu) at 40°C set point is 10°C as shown in figure 2 below.

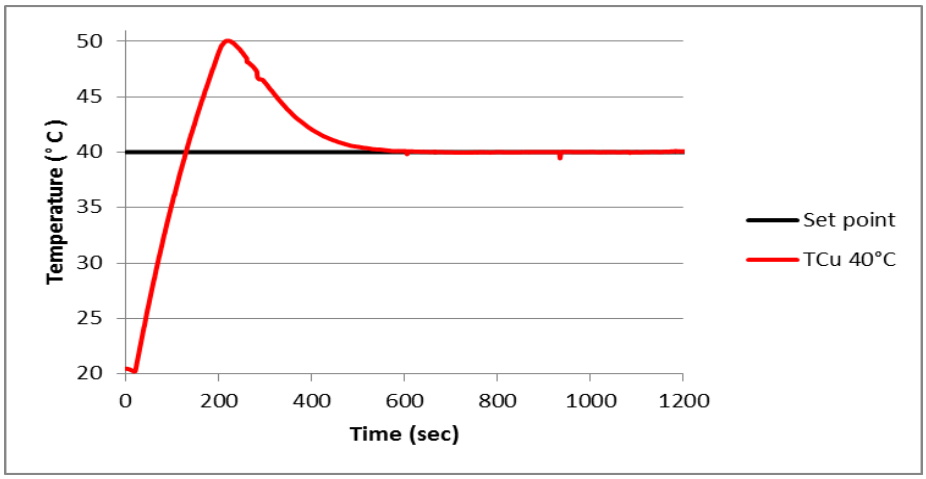

Figure 2: The copper temperature (TCu) behaviour at 40°C set point using PID parameters (P = 0.8, I = 50, D = 0) when applying constant temperature profile

This overshoot can be reduced by tuning the PID controller and selecting the appropriate tuning values which will give as low overshoot as possible. The importance of applying constant temperature profiles with no overshoot is to perform thermal experiments on living cells. The living cells are very sensitive to temperature and cannot survive under high temperature conditions.

The identification of cells using sensor devices is commonly based on electronic read-out [28, 29], microbalances [19], or microfluidic techniques [30]. For example, quartz-crystal microbalance (QCM) is a label-free technique based on mass loading. The heart of this technique is the quartz crystal. By monitoring the crystal resonance frequency it is possible to determine mass changes and, thus, to study different interfacial processes in thin films, to determine species transport, adsorption kinetics and growth. Also, piezoelectric quartz crystals have been applied in adsorption kinetic studies. In this way, protein adsorption kinetics and metals like copper, among others, have been investigated [27]. However, these

kinds of techniques require advanced equipment; thus, a simple and low-cost device that allowing distinguishing cells on basis of their size, shape or membrane functionalities is needed.

There are several examples show that the shape of cells and the structure can be related to certain diseases; the difference in the density of carbohydrate antigens of the ABO system (Blood grouping system) on the glycocalyx of erythrocytes determines the blood group and Rhesus factor of mammals [12, 13, 14]. Also, specific shapes of the erythrocytes can correlate with diseases such as sickle-cell anemia [12,15]. Sickle-cell anemia is one of the most common forms of sickle cell disease (SCD). SCD is a blood disorder, characterized by red blood cells that assume an abnormal and sickle shape as shown in figure 3 below.

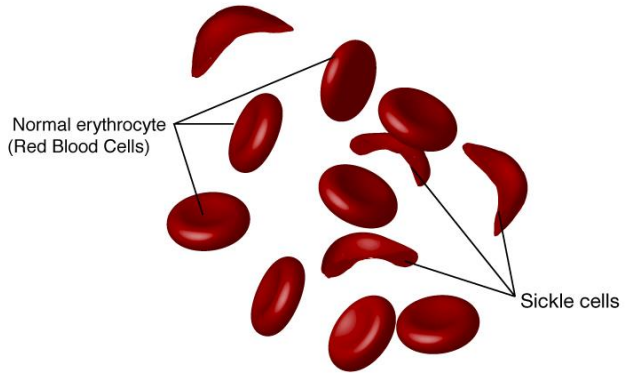

Figure 3: Normal red blood cells and Sickle cells [25]

Sickle cells contain abnormal hemoglobin called sickle hemoglobin or hemoglobin S that causes the cells to develop a sickle shape [24].

Sickle cells are rigid and sticky. They tend to block blood flow in the blood vessels of the limbs and organs. Blocked blood flow can cause organ damage, it can also raise the risk for infection [24].

Using surface-imprinted polyurethane (SIPs) layers on quartz-crystal microbalances (QCM), dickert's group succeeded in ABO phenotyping of erythrocytes without any labeling [12,19]. The greatest discrimination upon binding of AB-cells was found for AB-imprinted SIPs, presenting a 25% response when exposed to O-type cells as compared to the 100% response [12].

The sensor cell will focus on two different types of macrophages: rat alveolar macrophages (cell line NR8383) and mouse leukemic monocyte macrophages (cell line RAW 264.7), since the shape and membrane groups of macrophages can be correlated with cardiovascular diseases. For example, microphages in atherosclerosis patients show different antigens on their membranes comparing to macrophages of healthy persons [16, 17]. This has been recently described in the work on the selective identification of macrophages and cancer cells based on thermal transport through surface-imprinted polymer layers [12].

The advantages of using SIPs include strong binding capacity, inexpensive synthesis, thermal and chemical stability [9].

In order to perform thermal resistance measurements on living cells, (SIPs) layers will be used, SIP layer will be attached on top of aluminum substrate and target cells will be added to be bound on the SIP layer as shown in figure 4 below, the SIP-aluminum sample will be attached to the copper contact of the sensor setup .

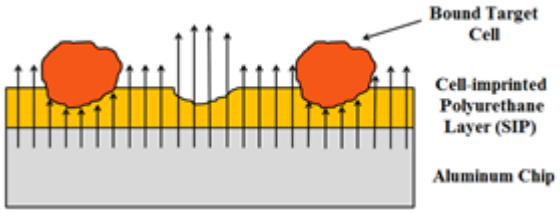

Figure 4: Cell binding to the binding cavities of the SIP on aluminum substrate [12]

The main goal of this project is to use the thermal sensor-device to perform Rth measurements on living cells; this can be done by reducing the high overshoot temperature values that appear when applying constant temperature profiles. The project also aims to evaluate the thermal measuring system and to detect DNA denaturation on different samples.

In this project, the thermal sensor-device can be used to measure Rth of (ds) DNA samples to detect denaturation; this is done by heating the samples by means of PID controller using temperature ramping profile. Also the setup can be used to measure Rth of living cells by applying constant temperature profile at 37°C after removing the overshoot in temperature. Therefore, the measurement setup will be able to measure Rth not only for DNA samples, but also on different living cells.

The applications of biosensors are often essential in the area of health care, allowing a better approximation of the metabolic state of patients. Also, a cheap, reliable and fast sensor is demanded, not only for routine monitoring in laboratories, but also with better patient contact, for example, in hospitals and operating rooms [21].

2. Methods and Materials

2.1 Measurement of the sensor cell

The sensor setup in figure 5 was used. The setup contains a flow cell with an inner volume 110 µl, the copper and liquid temperature are monitored using two thermocouple electrodes, one electrode is placed at a position backside of the copper lid, the other is positioned in the center of the flow cell at a distance 1.7 mm from the surface of the chip. A 10Ω power resistor is tightly placed on the copper lid as a heating source via the PID controller connected to the resistor. The sample containing DNA or SIPs is placed on the copper and exposed to 1 × phosphate-buffered saline solution (PBS) buffer. The contact area between the sample and the liquid is 28 mm^2 by using an O-ring seal. The heat will be transferred from the copper to the liquid through the sample. Conductive silver paint is used to reduce the heat loss between the copper and the sample.

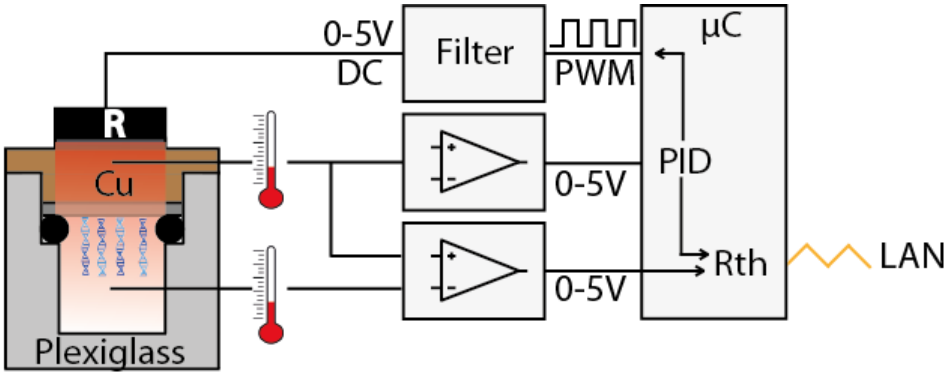

Figure 5: Block diagram of the sensor cell system [7]

2.2 Readout Device

The main platform in device development is the open source Arduino UNO development board as shown in figure 6. This low cost microcontroller has 14 digital input/output pins and based on the 8-bit Atmel ATmega328 microcontroller with 32KB of program memory. For better (Rth) measurement both the applied thermal power to the lid and the difference in temperature between the copper and liquid need to be determined. The resolution of the system is 10 bit resolution; 1024 discrete levels and the voltage ranges that can be read are between 0 and 5 V.

Figure 6: Arduino UNO Microcontroller [8]

The voltage generated by the copper and liquid thermocouple was amplified by using an instrumentation amplifier with a gain was set at 2500 and an offset voltage equals to 2.5 V. Differential voltages between -1.08mV and +1.08mV are amplified to the range of 0 to 5 V. The resolution of the differential voltage of 2.11 V between the both thermocouples is achieved, and a temperature resolution of 0.05°C within a differential range of -26°C to +26°C. The gain set of the non-inverting amplifier is 980 which amplifies the voltage of the copper signal and then processed into a PID controller.

The maximum temperature is set at 124°C with a resolution of 0.12°C. Both voltage signals are averaged over 1000 measurements in the microcontroller to improve the resolution. The applied power can be regulated precisely by the PID control. A passive filter (resistor-capacitor) is used to convert the pulse-width modulation (PWM) signal to a direct current (DC) voltage. The maximum applied power is 2.5 W since the DC output range is set between 0 to 5 V as expressed in the following formula:

$$\mathrm{P} = \frac{V^2}{R} = \frac{V^2}{10\Omega}$$

The heat transfer resistance (Rth) of the DNA samples can be described as:

$$Rth = \frac{\text{Difference between copper and liquid temperature}}{\text{The applied power to the resistor}}$$

2.3 DNA Sample preparation

2.3.1 Preparation of diamond-coated electrodes

Nanocrystalline diamond (NCD) films with thicknesses of ~ 100 nm and grain sizes of 50 nm were grown on a 2-inch doped (1–2 Ω cm) p-type crystalline silicon wafer (100), using microwave plasma-enhanced chemical vapour deposition (MPECVD) in ASTEX reactor equipped with a 2.45 GHz microwave generator. To achieve a good electrical conductivity in the range of 1 Ω cm, Chemical vapour deposition (CVD) was done with an admixture of trimethyl borane (B(CH3)3) to the CH4 gas with a concentration ratio of 200 ppm B/C to dope the NCD with boron [31]. The substrates were diced into samples of 10 mm by 10 mm after deposition [5].

2.3.2 DNA Functionalization of the electrodes

Photochemical attachment of 10-undecenoic acid to hydrogen terminated NCD was performed using ultra-violet radiation (254 nm, 265 mW-cm-2) for 20 hours under nitrogen atmosphere. NH2-terminated ssDNA (36-mer with the sequence 5'–NH2-C6H12-AAA-AAA-ACC-CCT-GCA-GCC-CAT-GTA-TAC-CCC-CGA-ACC-3') was covalently linked to the carboxylic (COOH) group of the 10-undecenoic acid using 1-ethyl-3-(3-dimethylaminopropyl) carbodiimide (EDC) coupling. The total amount of probe (ss) DNA used to functionalize 1cm2 of electrode surface was 300pmol. Non-specifically bound DNA is removed using 2 × saline sodium citrate (SSC) + 0.5 % sodium dodecyl sulphate (SDS) for 30 minutes. Finally, the sample is rinsed with phosphate buffered saline (PBS) of pH 7.2 and stored in PBS at 4°C [5].

2.3.3 Hybridization with target DNA

The ss-DNA probe was hybridized with 600 pmol of Alexa-488-labelled 29-mer target DNA. A 6 µl target DNA is mixed with 14 µl 1× PCR buffer and added to the ssDNA-modified NCD sample for 2 hours at 35°C. Non-specifically bound DNA is removed 2 × SSC + 0.5% SDS buffer for 30 minutes at room temperature, followed by 5 minutes washing step with 0.2 × SSC buffer at 30°C. Then the sample was washed with 0.2 × SSC buffer at room temperature. Finally, the sample was rinsed with PBS of pH 7.2 and stored in PBS at 4°C [5].

2.4 Living cells preparation

2.4.1 Preparing cell-imprinted polyurethane layers

Polyurethane layers were made by dissolving 122 mg of 4.4'- diisocyanatodiphenylmethane, 222-mg of bisphenol A, and 25 mg of phloroglucinol in 500 µl of anhydrous tetrahydrofuran (THF). The mixture was stirred at 65°C under nitrogen atmosphere for 200 minutes until the solution reached its gelling level. The solution was diluted in a 1 : 5 ratio in THF and spin-coated for 1 minute at 2000 rpm onto 1 cm^2 aluminum substrates. The average thickness of the polyurethane layers was around 1.2µm ± 0.1 µm. Polydimethylsiloxane (PDMS) stamps were covered with cells to stamp the cells into the polyutethane layer. Cell suspension in PBS of 400µl was applied to the PDMS. The excess fluid was removed after 50 seconds of sedimentation time by spinning at 3000 rpm for 1 minute to create a solid monolayer of cells on the stamp surface. The covered stamp was pressed under 70 Pa pressure onto the polyurethane layer and cured under nitrogen atmosphere for 18 hours at 65°C. Then, the stamp was removed from the surface. The template cells were washed off from the layer by rinsing the surface with PBS and 0.1% Sodium dodecylsulfate (SDS) solution, leaving behind selective cavities on the surface of the polyurethane layer. For assessing specificity, non-imprinted polymer layers were used, the layers were made in the same way as the imprinted layers. However, no template cells were used during PDMS stamping [12].

2.4.2 Cell Culturing

Mouse leukemic monocyte macrophage RAW 264.7 cells (American-type culture collection ATCC: TIP-71) and rat alveolar macrophage NR8383 CELLS (ATCC: CRL-2192) were cultured in Roswell Park Memorial Institute medium (RPMI medium, Lonza Braine S.A., Braine-1'Alleud, Belgium). The RPMI medium was exchanged with PBS in order to remove proteins of the culture medium in six washing steps. Cells were counted using a haemocytometer (VWR International, Leuven, Belgium) to determine the cell concentration in buffer medium. All ATCC cell cultures were ordered at LGC Standards S.a.r.l., Molsheim Cedex, France [12].

2.4.3 Characterization of SIP layers

SIP layers were synthesized with two spherical cell types, NR8383 cells (rat alveolar macrophages) with diameter of ≈ 25µm and RAW 264.7 cells (mouse leukemic monocyte macrophages) with a diameter of ≈ 15µm. An Axiovert 40 inverted optical microscope (Carl Zeiss, Jena, Germany) was used to perform optical analysis of the imprinted polyurethane [12].

3. Results and Discussion

3.1 System evaluation

Different measurement profiles have been performed, to evaluate the sensor system and how accurate is the system.

3.1.1 Ramping profile

To evaluate the sensor system by performing ramping temperature cycles, the copper temperature is the most significant factor to be studied, because it is directly dependent on the heating source of the sensor cell, but it is not the case for the liquid temperature, since it is sample-dependent, so it is not relevant to study the liquid temperature behaviour with respect to the applied set point temperature.

To determine the deviation between both copper temperature (TCu) and set point**,** temperature ramping profile have been performed by heating and cooling the (ss) DNA sample between 25° C and 80°C at a rate of 1°C/min for 28 hours. This shows how the copper temperature will correspond to the set point temperature. Figure 7 shows the copper temperature and set point behaviour during the ramping profile and the measurement has been done for 7 hours. The PID control parameters were set as P = 0.8, I = 50, D = 0 ; these values are suitable for applying ramping profiles since the copper temperature corresponds finely to the set point with small difference in temperature.

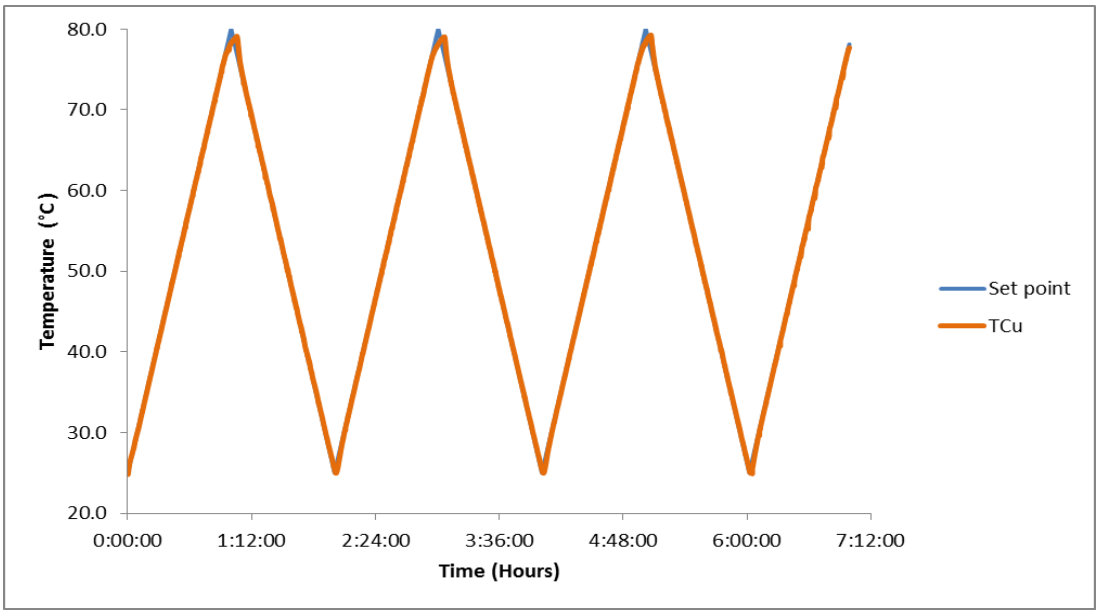

Figure 7: The copper temperature behaviour on (ss) DNA sample during ramping profile using PID parameters (P = 0.8, I = 50, D = 0)

The average temperature difference between copper and set point during heating runs of the applied ramping profile over 28 hours is shown in figure 8, where ΔT = set point temperature (Tset) - Copper temperature (TCu) .

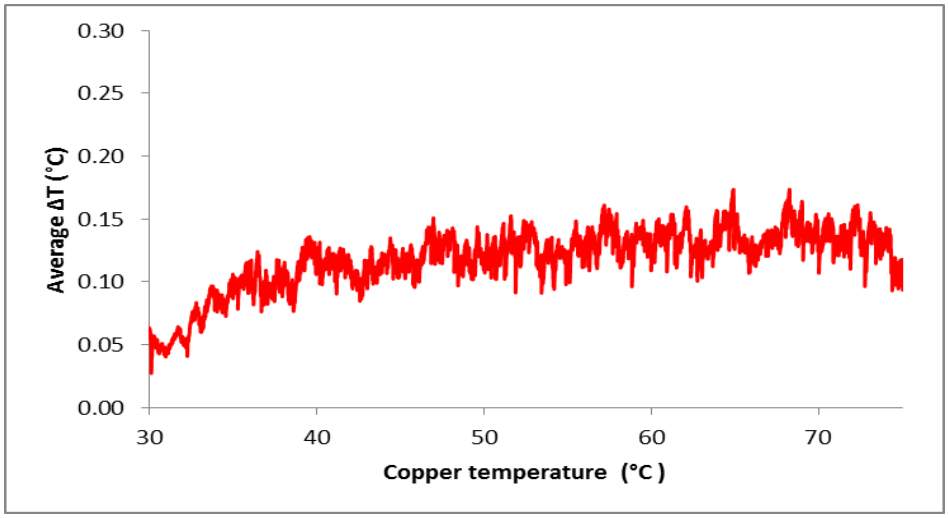

Figure 8: Average temperature difference between copper and set point versus copper temperature

Figure 8 summarized the data obtained from applying 12 heating runs over 28 hours of the applied ramping cycles. The copper temperature follows the set point temperature below 75°C with a maximum error of 0.15°C. It should be stated that the applied power is not sufficient to heat above 75°C.

3.1.2 Constant temperature profile

The PID control parameters were set as P = 0.8, I = 50, D = 0, the same parameters that have been used in applying ramping profile. A constant profile temperature is applied at 5 different set point values of (30°, 40°, 50°, 60° and 70°C) and monitoring the copper temperature behaviours at each value have been obtained as in figure 9 below. This allows determining the overshoot values at different temperature profiles.

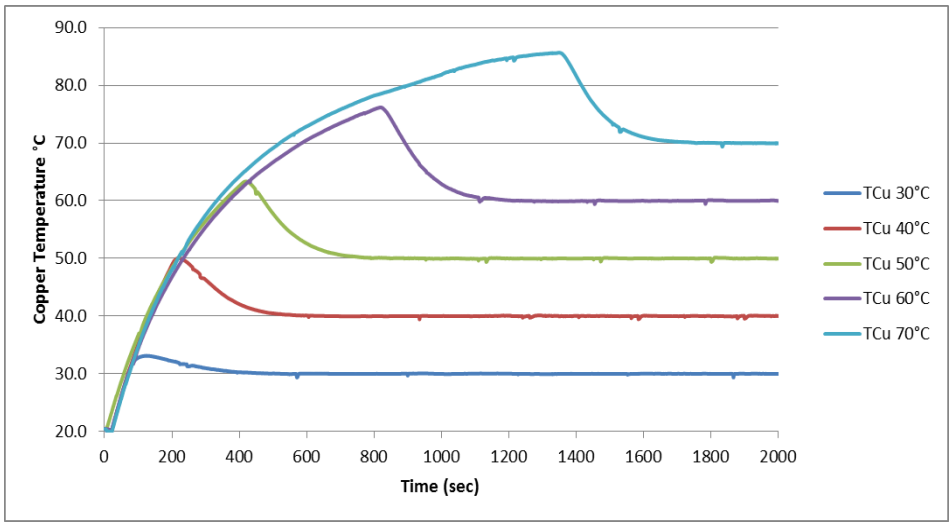

Figure 9: Five different Copper temperature behaviours against time in seconds

From figure 9, each curve represents the copper temperature behaviour at certain set point value, all the temperature curves are nicely follow each other at a common starting point of

20°C, each temperature curve require a certain time until it becomes stable at constant temperature; this is called the rise time. For higher copper temperatures, the rise time will be longer. From figure 9, the rise time for each temperature curve can be determined, table 1 below shows the rise time for each copper temperature curve.

Table 1: The rise time for the five different copper temperature curves

Set point (°C)	30	40	50	60	70
Rise time (in min)	8	11	14	20	29

The peak temperatures of each curve can be determined, after this point the temperature starts to decrease until it reaches the saturation temperature level, the peak temperature points and the overshoot values of each temperature curves are shown in table 2. The overshoot can be obtained by calculating the difference between peak temperatures and the set points. So it is clear that the overshoot in temperature increases as the copper temperature increases.

Table 2: The peak temperature and the overshoot values at the different copper temperature

Set point (°C)	**Peak temperature (°C)**	**Overshoot (°C)**
30	33	3.0
40	50	10
50	63.5	13.5
60	76	16
70	86	16

The importance of studying the overshoot temperature is to know the accuracy of the system and to determine if the system can be applicable to perform measurements on living cells.

The set point for living cells measurements has to be 37°C and the maximum overshoot in copper temperature has to less than 1°C, otherwise the living cells would die. From table 2, the overshoot value of the set point 40°C is 10°C which is extremely high and the system is not ready to perform living cells measurements yet.

Monitoring the copper temperature behaviour at a certain set point temperature allows determining the noise level of the temperature. From figure 10, the noise level of the copper temperature curve at 37°C set point is 0.10°C.

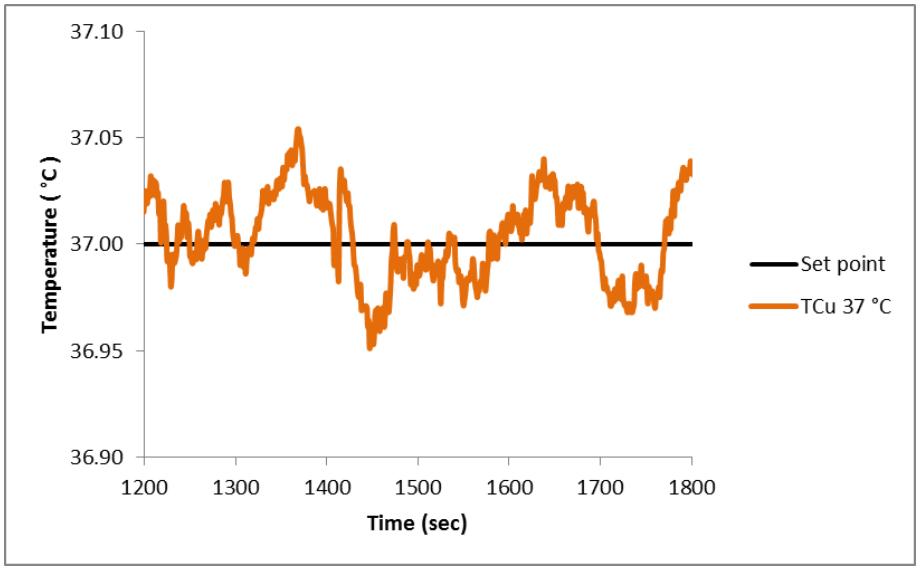

Fig 10: The noise level of the copper temperature at 37°C set point

The overshoot in copper temperature is extremely high as described before in table 2 and in order to perform living cells measurements, the overshoot in copper temperature has to be reduced.

This measurement system is still not accurate enough to perform thermal experiments on living cells, due to the high overshoot and the noise of the temperature values. Reducing the high overshoot temperature will be described in section (3.2. System optimization).

3.2 System Optimization

The PID controller parameters have the main influence on the copper temperature behaviour with respect to the set point temperature. As discussed in section 3.1.2, the overshoot values in copper temperature are extremely high when using the PID parameters (P = 0.8, I = 50, D = 0) in applying constant temperature profiles.

To remove these high overshoot values that appear in constant temperature profiles, Ziegler-Nichols method will be used to obtain optimal parameter values of the PID controller.

3.2.1 Tuning PID parameters using Ziegler –Nichols method

To determine the PID parameters using Ziegler-Nichols method, a unit step input has to be applied, as shown in figure 11, and then the response of the system will be obtained.

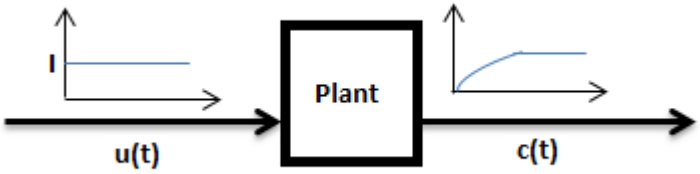

Figure 11: Unit-step response of a plant

The response of the output curve can be characterized by two constants, delay time (L) and time constant (T) as shown in figure 12, those two constants can be determined by plotting a tangent line at the inflection point of the response curve and determining the intersection points of the line c(t) = K with the tangent line and the time axis.

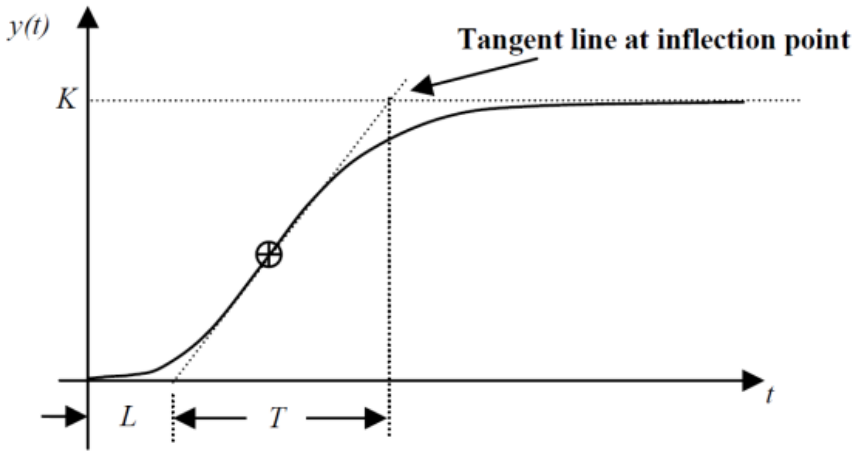

Figure 12: Ziegler-Nichols output response curve [18]

After determining the values of L and T of the output response curve, the PID parameters can be obtained using Ziegler-Nichols tuning formulas as shown in table 3 below.

Table 3: Ziegler-Nichols tuning formulas based on step response of plant [18]

Type of controller	P	I	D
P	T/L	∞	0
PI	0.9 (T/L)	L/0.3	0
PID	1.2(T/L)	2L	0.5L

Unit step response experiment has been done by applying a constant input voltage and the output response curve (copper temperature) is shown in figure 13.

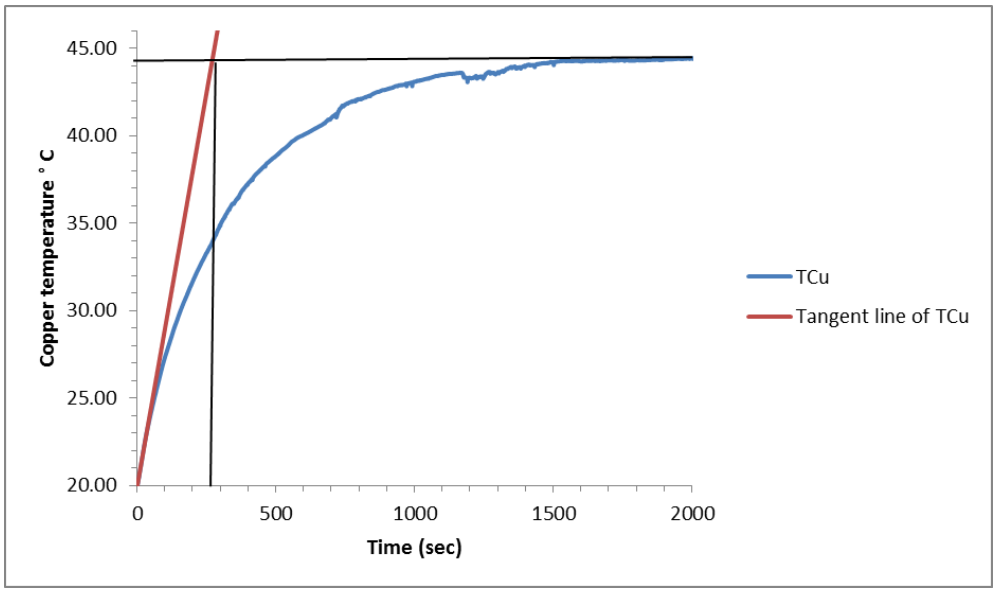

Figure 13: Output response curve of TCu using constant input voltage

T and L constants can be determined based on drawing a tangent line of the TCu curve. The value of constant L is 2 seconds and T is 271 seconds. Using Ziegler–Nichols table, the PID parameters based on PI controller were obtained and the values are as follows P = 122, I = 6.66 and D = 0. The use of PI controller is more common than the PID controller, since the derivative action (D) is sensitive to the noise.

The new set of PID parameters (P = 122, I = 6.66, D = 0) have been tested by applying constant temperature profile and the output response curve of TCu is shown in figure 14.

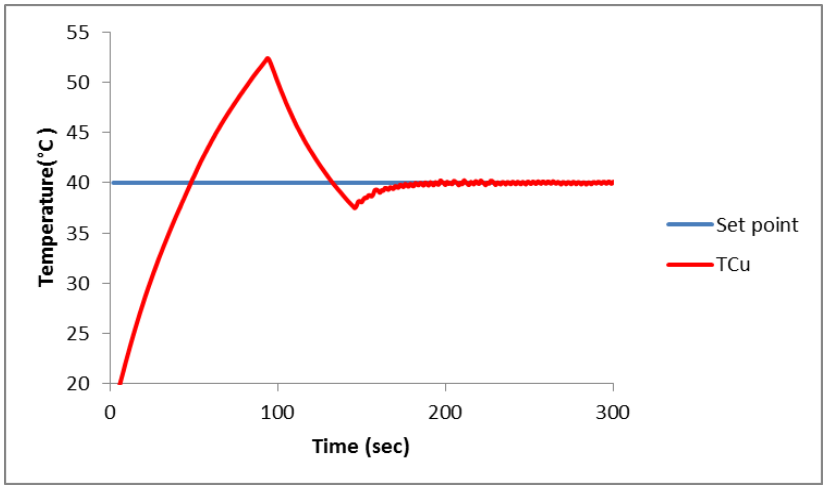

Figure 14: The TCu behaviour using Ziegler-Nichols PID parameters (P = 122, I = 6.66, D = 0)

The overshoot of TCu at 40°C set point using Ziegler-Nichols method is very high (12.5°C), this is due to that the response curve of the applied unit step response (figure 13) does not exhibit an S-shaped curve, Thus, resulting in a very large value of P parameter.

Since Ziegler-Nichols method does not exhibit the desired output response, another approach has been applied based using Lambda method.

3.2.2 Tuning PID parameters using Lambda method [22, 23]

The Lambda tuning rules offer a robust alternative to tuning rules aiming for speed, like Ziegler-Nichols and Cohen-Coon.

Ziegler-Nichols and Cohen-Coon rules aim for quarter-amplitude damping, while Lambda tuning rules aim for a first-order lag plus dead time response to a set point change.

To determine the PID parameters using Lambda tuning method, a unit step input has to be applied, and then the response of the system will be obtained as in figure 15. The same as in Ziegler-Nichols steps.

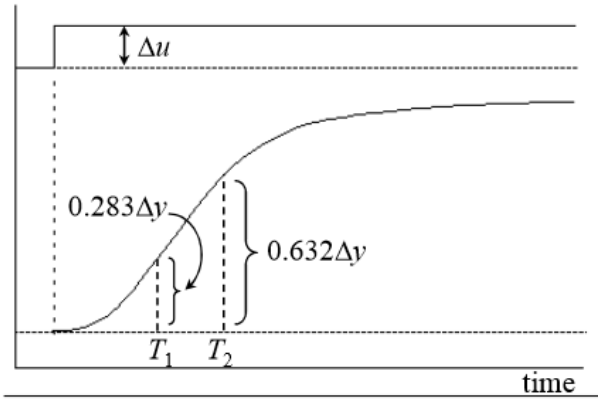

Figure 15: Output response using Lambda method

The response of the output curve is characterized by three constants:

- Process gain (Gp)
- Process time constant (τp)
- Process dead time (Td)

The three parameters can be determined based on the output response curve by the following formulas:

$$Gp = \frac{\Delta y}{\Delta u} \quad (1)$$

$$\tau p = 1.5\ (T2 - T1) \quad (2)$$

$$Td = T2 - \tau p \quad (3)$$

From the output response curve of TCu as shown in figure 16, the three parameters can be determined.

To evaluate the "three constants" as shown in formula (1), (2) and (3), T1 and T2 should be determined based on the output curve of TCu as shown in figure 15 , the value of T1 is 93 seconds (1.55 minutes) at 26.93°C and T2 is 320 seconds (5.33 minutes) at 35.48°C. The unit step input voltage where set at 150 (Δu = 150) and the output change is Δy = 24.5.

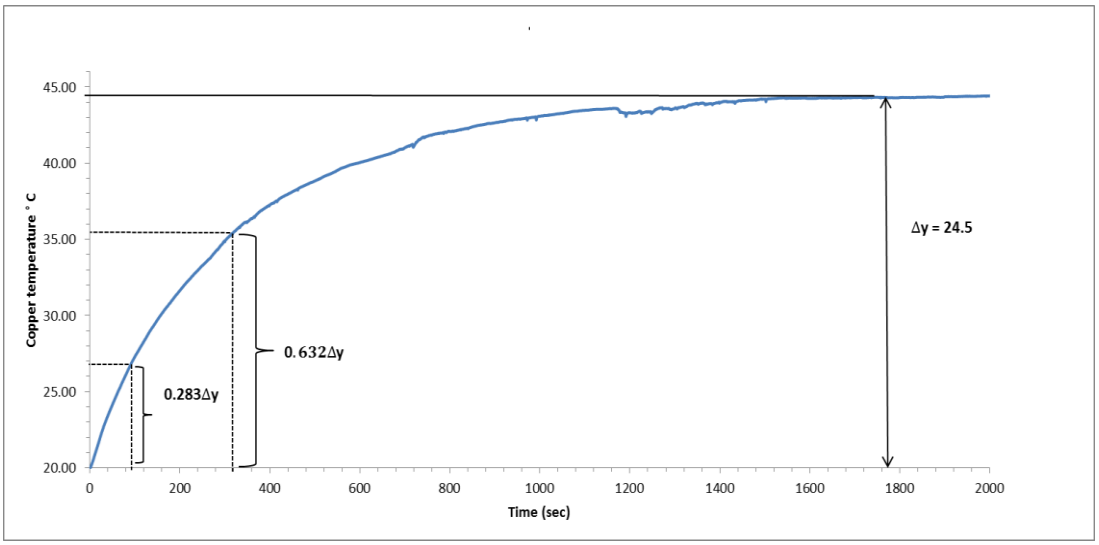

Figure 16: Output response curve of TCu using Lambda method

Now, the three constants can be determined using formulas (1), (2) and (3):

- $Gp = \frac{\Delta y}{\Delta u} = \frac{24.5}{150} = 0.163$
- $\tau p = 1.5\ (T2 - T1) = 1.5\ (5.33 - 1.55) = 5.675$
- $Td = T2 - \tau p = 5.33 - 5.675 = -0.345$

After determining the three parameters Gp, τp and Td, the controller parameters can be obtained using Lambda relations given in the following formulas:

(Where λ is the desired closed-loop time constant and typically 2 to 3 times the process constant)

$$P = \frac{2\tau p + Td}{2Gp - (\lambda + Td)} \quad (4)$$

$$I = \tau p + Td/2 \quad (5)$$

$$D = \frac{\tau p * Td}{2\tau p + Td} \quad (6)$$

The PID parameters were obtained and the values are as follows P = 1.03, I = 5.50, and D = 0.177.

The new set of PID parameters (P = 1.03, I = 5.50, D = 0.177) have been tested by applying constant temperature profile at 37°C and the output response curve of TCu is shown in figure 17.

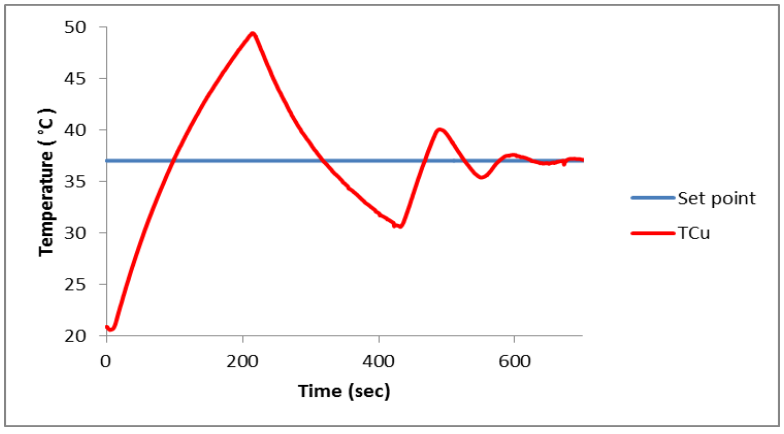

Figure 17: The TCu behaviour using Lambda PID parameters (P = 1.03, I = 5.05, D = 0.177)

The overshoot of TCu at 37°C set point Lambda method is very high (12.5°C), this is due to that that the output response curve of TCu has a very low delay time (not S-shaped).

Since Ziegler-Nichols and Lambda methods do not exhibit the desired output response, another approach has been applied based using practical experiments.

3.2.3 Tuning PID parameters based on practical experiments

Adjusting the PID parameter values have been done several times under different PID parameters on blank aluminum sample. In figure 18 below, constant temperature measurements at 37°C set point have been done using three different PID parameters as follows PID (1): P = 0.80, I = 50, D = 0, PID (2): P = 0.40, I = 50, D = 0, and PID (3): P = 0.55, I = 70, D = 0. Note that PID (1) parameters (P = 0.80, I = 50, D = 0) are used for applying temperature ramping profile.

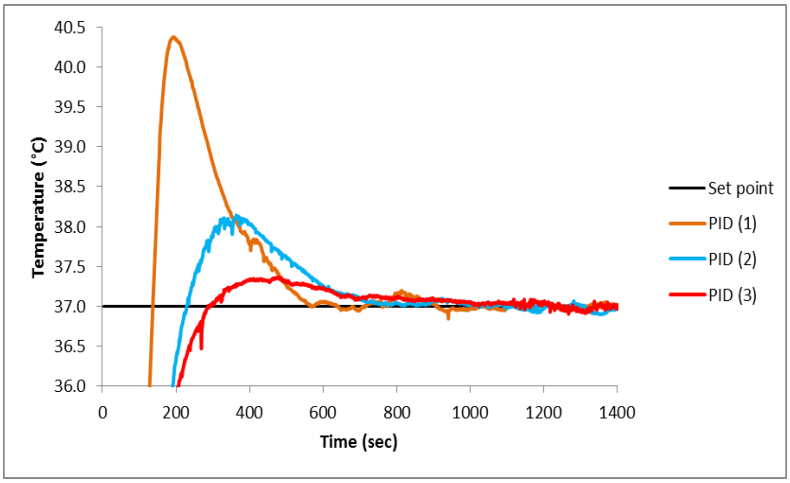

Figure 18: Copper temperature behaviour using three different PID parameters at 37°C set point

The overshoot values of the copper temperature at 37°C set point using the three different PID parameters are shown in table 4 below.

Table 4: The overshoot of TCu using three different PID parameters at 37° set point

PID Parameters	PID (1)	PID (2)	PID(3)
Overshoot °C	3.37°	1.09°	**0.34°**

The overshoot of the TCu using PID (3) is 0.34°C which is appropriate to be used in performing living cells measurements since it is lower than 1°C.

The new set of parameters PID (3) (P = 0.55, I = 70, D = 0) will be used to apply new constant temperature profiles at 5 different set points values 30°, 40°, 50°, 60° and 70 °C (the same as in section 3.1.2. Constant temperature profile). Figure 19 below, shows the overshoot of the copper temperature curves at different set points using the new PID parameters. Also, the set point temperature profile has been done using PID (2) (P = 0.40, I = 50, D = 0) as shown in the supplemental information section.

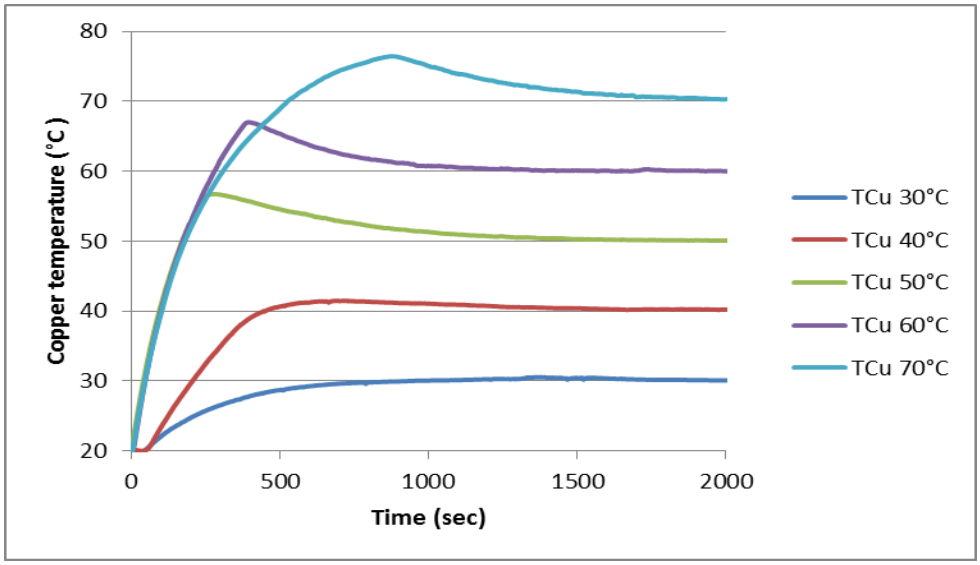

Figure 19: Five different Copper temperature behaviours against time in seconds using the new PID (3) parameters (P = 0.55, I = 70, D = 0)

From the figure above, the rise time for each temperature curve can be determined, table 5 below shows the rise time for each copper temperature curve

Table 5: The rise time for the five different copper temperature curves using PID (3)

Set point (°C)	30	40	50	60	70
Rise time (in min)	15	23	20	19	30

Table 6 shows the overshoot values at different temperature set points for the three different PID controllers PID (1), PID (2) and PID (3).

Table 6: Comparison between the overshoot values using three different PID parameters

Set point (°C)	Overshoot (°C) using old PID (1) Parameters (P = 0.8, I = 50, D = 0)	Overshoot (°C) using PID(2) Parameters (P = 0.4, I = 50, D = 0)	**Overshoot (°C) using PID (3) Parameters (P = 0.4, I = 50, D = 0)**
30	3.0	0.70	**0.30**
40	10.0	1.40	**1.39**
50	13.5	9.80	**6.55**
60	16.0	12.30	**7.00**
70	16.0	10.70	**6.42**

Testing the new PID parameters (P = 0.55, I = 70, D = 0) at 37°C set point have been performed on blank aluminum sample, this allows to determine the overshoot of the TCu. Figure 20 below, shows the TCu behaviour at 37°C set point temperature. During the measurements, the aluminum sample is exposed to PBS buffer around 1400 seconds of the experiment to monitor the TCu response when flowing PBS buffer.

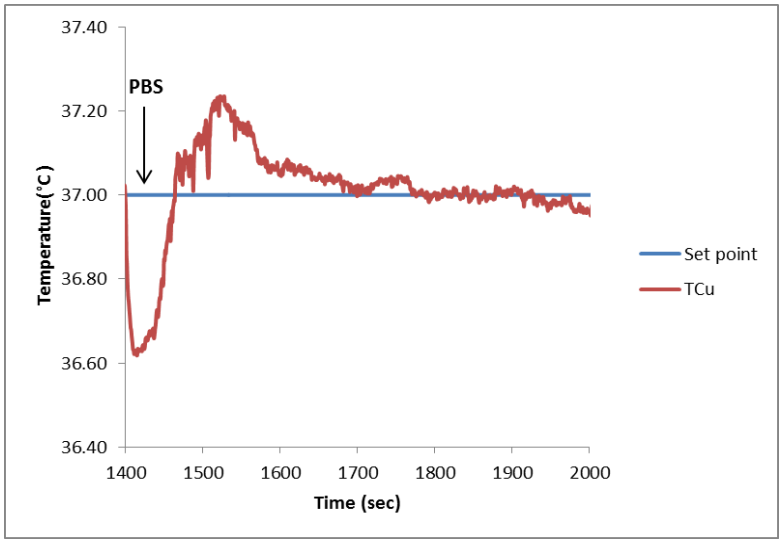

Figure 20: The copper temperature behaviour at 37°C set point using the new PID parameters (P = 0.55, I = 70, D = 0) on blank aluminum sample

From figure 20, after flowing PBS buffer into the liquid reservoir of the sensor cell using manual syringe, the TCu falls to 36.6°C, then, it starts to rise rapidly to about 37.24°C by means of the PID controller to compensate this temperature drop.

The noise level of the copper temperature at 37°C set point using PID (2) parameters (P = 0.40, I = 50, D = 0) and PID (3) parameters (P = 0.55, I = 70, D = 0) on a blank aluminum substrate is shown in figure 21 below.

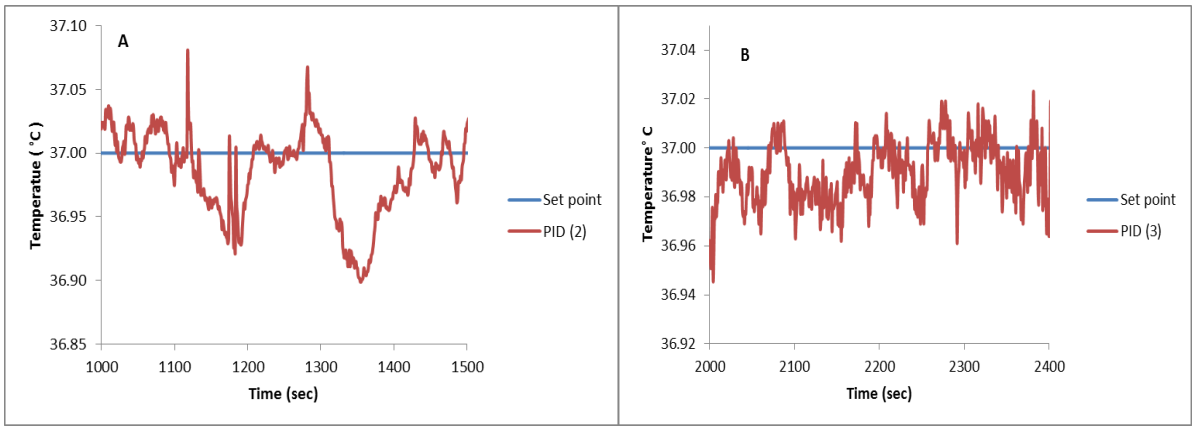

Figure 21: The noise level of the TCu at 37°C set point using A) PID (2) and B) PID (3)

The noise of TCu using PID (2) is around 0.18°C as shown in figure 19 A. Also, the noise of TCu using PID (3) at 37°C set point is laid between 36.95°C and 37.10°C which is around 0.07°C.

Table 7 below summarizes the data obtained with three PID parameters at 37°C set point.

Table 7: Comparison between the overshoot, noise and rise time using different PID parameters at 37°C set point.

PID parameters	Maximum overshoot(°C)	Maximum noise level(°C)	Rise time (in min)
PID (1) parameters (P = 0.80, I = 50, D = 0)	3.37	≈ 0.10°C	≈ 9.0
PID (2) parameters (P = 0.40, I = 50, D = 0)	1.09	≈0.18°C	≈ 12.5
PID (3) parameters (P = 0.55 , I = 70, D = 0)	**0.34**	**≈ 0.07°C**	**≈ 16.0**

From table 7, the maximum overshoot value of the set point 37°C is 0.34°C using PID (3) parameters which is smaller than using PID (2) and PID (3) and suitable to perform living cells measurements. Also, the maximum noise level using PID (3) is around 0.07°C and lower than the other PID parameters. However, using PID (3) parameters, the rise time is longer comparing to PID (1) or PID (2). This is due to that PID (3) has higher (I) value than the other controllers.

The importance of studying the overshoot of TCu using aluminum substrate is that the aluminum covered with a SIP layer will be the central element where the living cells will be added to be bound on top of the SIP layer. Then, the living cells Rth measurements can be performed at 37°C using the new set of PID parameters (P = 0.55, I = 70, D = 0).

So, the thermal sensor device will be used to perform Rth measurements on both DNA samples (based on silicon substrate) and living cells (based on aluminum substrate). For DNA measurements, the temperature ramping profiles using PID parameters (P = 0.8, I = 50, D = 0) will be applied. And for living cells measurements, constant temperature profile at 37°C using the new PID parameters (P = 0.55, I = 70, D = 0) will be applied.

3.3 Thermal Resistance Measurements

3.3.1 DNA measurements

A denaturation experiment on a perfectly matched double stranded DNA sample is shown in figure 22 after applying temperature profile (heating/cooling cycles) to the (ds) DNA and (ss) DNA as shown in figure 23. The copper element that contains the DNA sample was heated up to 80 °C and cooled down to 25 °C at a rate of 1°C/min.

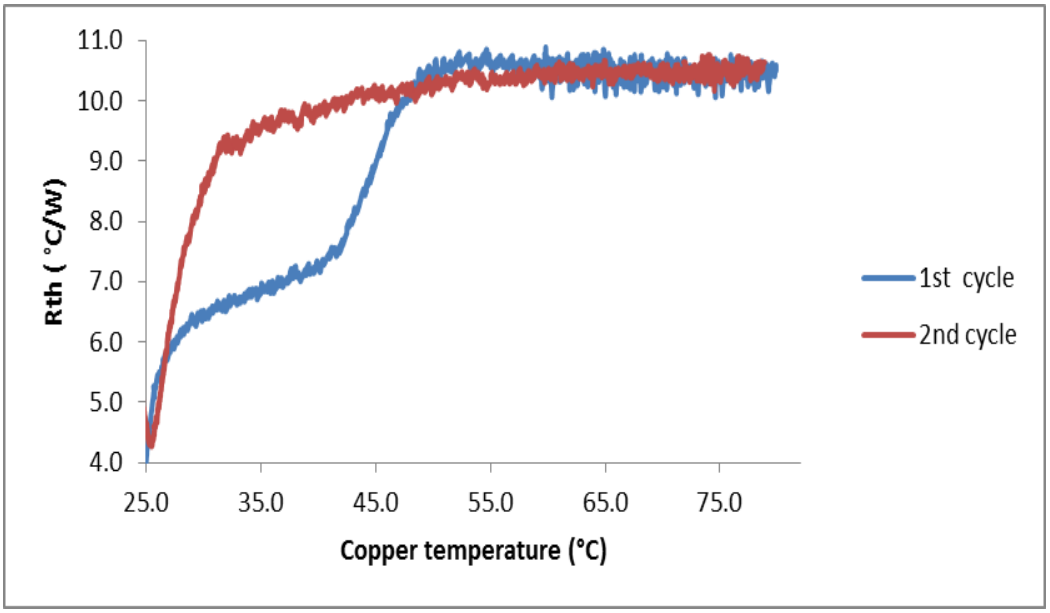

Figure 22 : Measured Rth versus copper temperature

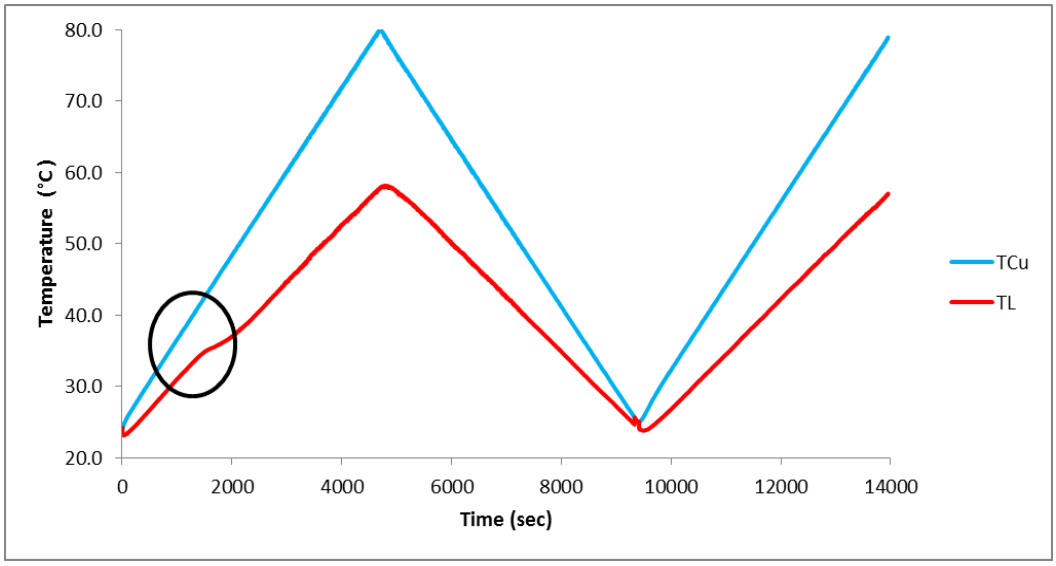

Figure 23: Applied ramping temperature profile

From the 1 cycle , Rth is shifted significantly from 6 to 10(°C/W) between 35° and 45° degrees of TCu , this shift is due to the DNA denaturation, in the second cycle the thermal resistance is around 10-11 (°C/W) and it corresponds to the (ss) DNA. This indicates that the

(ss) DNA has a higher Rth value (≈ 10.5 °C/W) than (ds) DNA (≈ 6.5 °C/W) and acts more like an insulating layer than the (ds) DNA.

During the first heating cycle of the measurement, an abnormal response of the liquid temperature (TL) happens around 35°C (the highlighted circle) as shown in figure 23, which was not existed during the second heating cycle, approving that this effect related to DNA denaturation based on exposing DNA samples to increasing temperature can lead to denaturation.

In order to prove that DNA denaturation can be induced due to increasing temperature, Figure 24 summarizes independent methods confirming that DNA denaturation can indeed be induced due to heating. The bottom-left of figure 24 shows the temperature difference (TCu-TL) with respect to TCu, the red curve corresponds to the (ds) DNA (first heating cycle) while the blue curve corresponds to the (ss) DNA (second heating cycle). Both curves differ in temperature below 45°C, this difference starts to vanish at 45°C and disappears completely at 65°C, where the denaturation process is completed.

The top-right of figure 24 shows the TCu with respect to the electrical voltage (V) that is needed to obtain the heating rate of 1°C/min. both curves match at temperature 45°C which is close to the temperature point where the Rth of the (ds) DNA starts to be saturated as in figure 22.

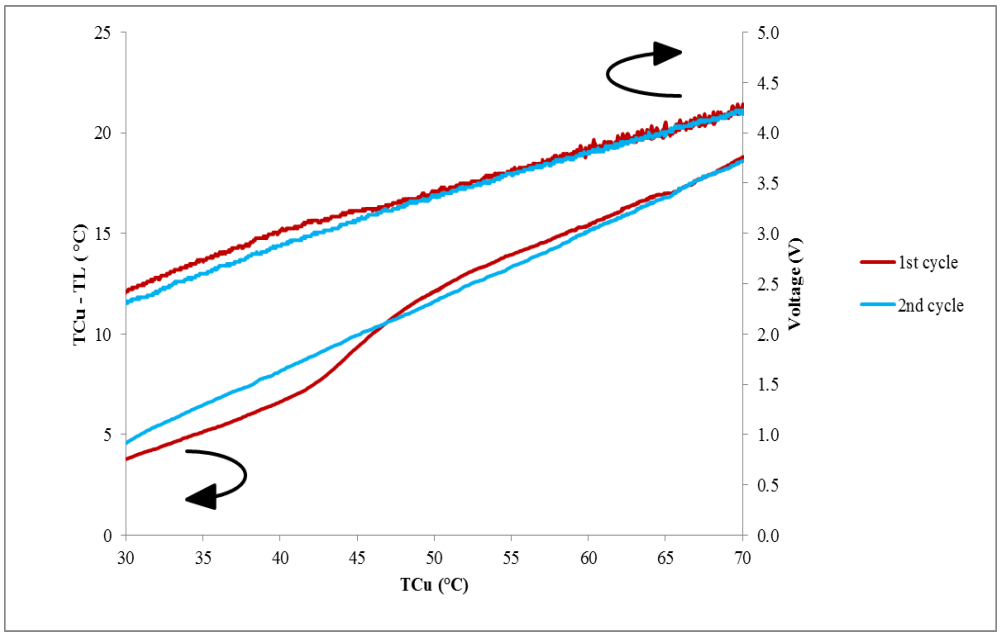

Figure 24: Temperature difference of copper and liquid with respect to TCu (bottom-left) together with the TCu with respect to the applied voltage (top-right).

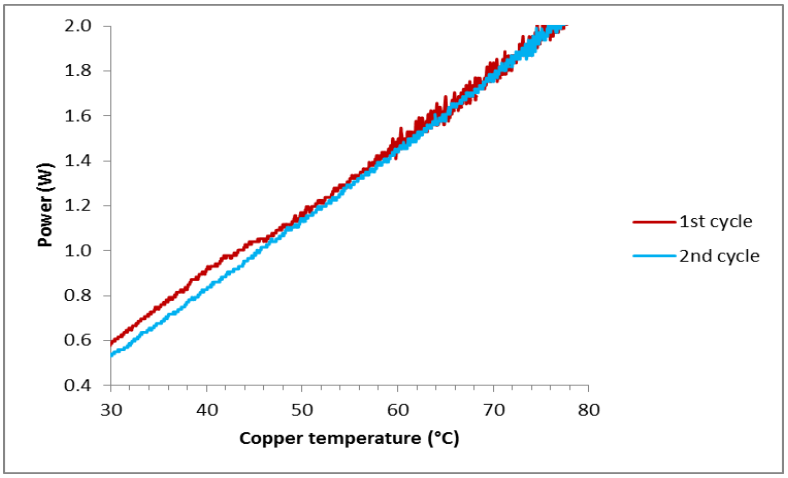

Figure 25: TCu with respect to the applied electrical power

Figure 25, shows the TCu with respect to the applied electrical power that is needed to obtain the heating rate of 1°C/min. Both curves match at temperature 50°C which is almost the same behaviour as in figure 24 including the temperature dependence of the electrical voltage. Below 50°C (before denaturation occurs), it is clear that (ds) DNA curve (1st cycle) has higher power value than (ss) DNA curve (2nd cycle). This is due to that the (ds) DNA is more thermally conductive and requires more power to obtain the desired set point temperature for TCu.

Another successful denaturation experiment is performed on perfectly matched DNA sample is shown in the supplemental information section.

3.3.2 SIP-Imprinted layer measurements

Rth measurements have been performed on blank aluminum substrate (reference sample) and SIP-imprinted layer on aluminum substrate at 37°C set point, this allows to determine the Rth value of the SIP layer. Figure 26 below shows the Rth response of both samples.

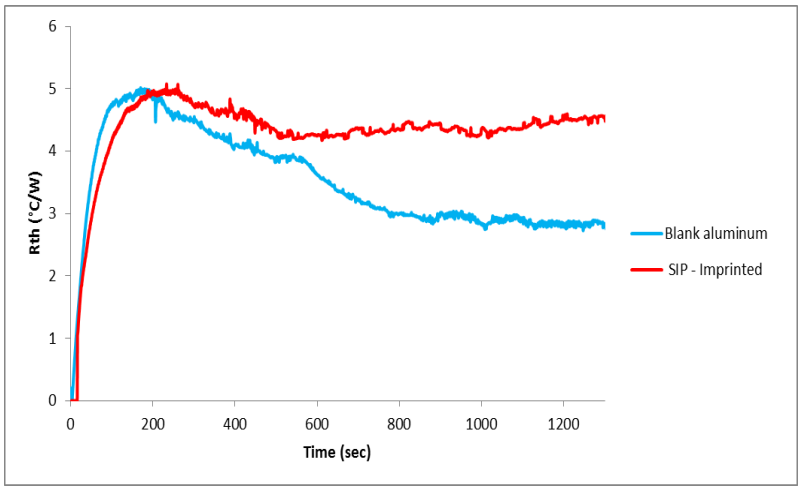

Figure 26: Measured Rth for blank aluminum and SIP-imprinted samples

From figure 26, the Rth curve of the blank aluminum stabilizes after 800 seconds at 3 (°C/W), while the Rth of the SIP-imprinted sample stabilizes at higher level around 4.50 (°C/W). This means that the SIP layer acts like a thermal insulating layer and its Rth value equals 1.5 (°C/W).

3.3.3 Living cells measurements

Figure 27 summarizes the living cells experiment that performed on NR8383 and RAW cells with RAW imprints. Exposing the RAW- imprinted layer on aluminum substrate to a RAW cell suspension is shown in Figure 27 A. First, the flow cell is filled with PBS buffer and the Rth is stable around Rth = 5 (°C/W). Next, RAW cells were exposed into the flow cell and the Rth shifted to a new equilibrium around 7.5 (°C/W) due to addition of these target cells. Then, the flow cell was flushed with SDS (sodium-dodelcyl sulphate solution) in order to distrust the target cells and lyse the cell membranes, resulting in a constant level of Rth. then, the flow cell was flushed with PBS buffer to remove the cells and Rth dropped to almost as the initial level value of 5.3 (°C/W).

Exposing the RAW-imprinted layer to an NR8383 cell suspension is shown in Figure 27 B. The Rth shifted from 6.7 to 8 (°C/W) due to addition of NR8382 cell suspension. Then, the flow cell was flushed with SDS, resulting in a small signal drift between 8.0 and 8.6 (°C/W). Finally, exposing PBS to the flow cell to remove the cells, resulting in Rth drop to 7.3(°C/W).

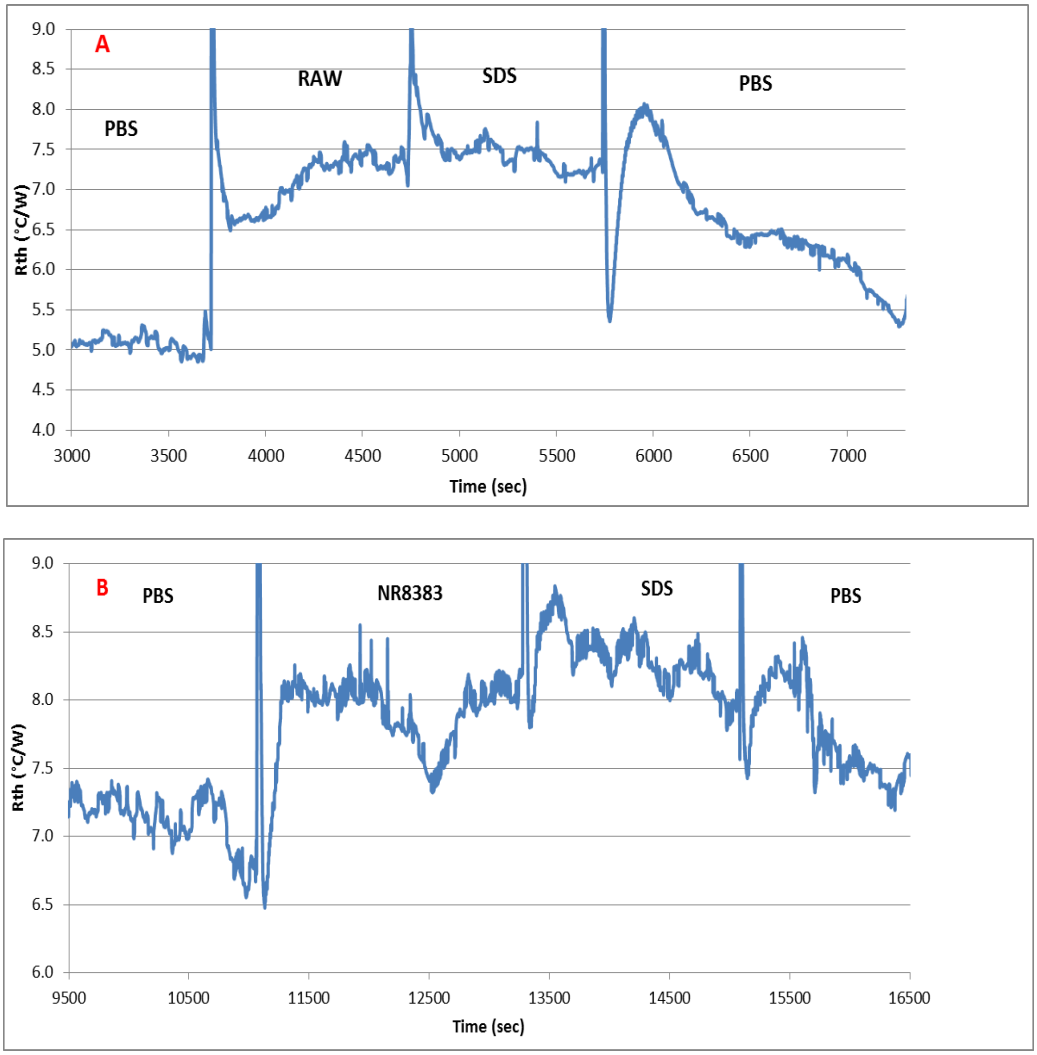

Figure 27: Thermal resistance experiment for macrophage detection, the sensor cell was used to discriminate between mouse (RAW 264.7) and rat (NR8383) macrophage cells. SIP layer was imprinted for RAW cells only and Rth response to both cells is obtained. (A) Recognition of RAW cells (target cells) with a RAW-imprinted SIP layer. (B) Time-dependent Rth response of a RAW-imprinted SIP layer when exposed to NR8383 cells

The increase in Rth due to exposing the RAW-imprinted SIP layer to the RAW cells (figure 27 A) is larger than the shift when exposing to NR8383 cells (Figure 27 B). This is due to binding of RAW cells in the imprinted cavities, while the increase of Rth when exposing to NR8383 is due to the presence of the cells in the flow cell and not related to the binding of cells in the imprinted cavities.

4. Conclusion

The hand-held thermal-sensor is a promising technique not only for detecting DNA denaturation, but also, for monitoring other molecular interactions such as cell-recognition by SIPs immobilized on aluminum substrate. Moreover, the thermal device is a low cost, fast, can be controlled using local-area network and allows for repetitive measurements.

During DNA denaturation, the Rth of the (ds) DNA has shifted significantly and proving that the (ds) DNA is more thermally conductive than (ss) DNA.

The overshoot in copper temperature has been reduced in order to perform thermal measurements on living cells at 37°C.

From the thermal measurements on living cells, the Rth has increased due to binding of target cells to the binding cavities of the SIP-imprinted on aluminum substrate. This can be used as a detection tool for cancer and cardiovascular diseases by imprinting several chips with a variety target cell types.

Impedance spectroscopy and quartz-crystal microbalances can also be used for cell-recognition by SIPs [19, 20]. However, the thermal sensor device is not dependent on the electrical conductivity or piezoelectric effects of the material [12]. From this point, a further study can be done to combine the thermal sensor device with an impedance spectroscopy or QCM in one powerful tool to study a wider number of properties related to the surface and interfacial processes.

References

1. Schon E A, Bonilla E and DiMauro S. *Mitochondrial DNA mutations and pathogenesis*. 1997 J. Bioenerg. Biomembr. 29 131-149

2. Dunning A M, Healey C S, Pharoah P D P, Teare M D, Ponder B A and Easton D F A. *A systematic review of genetic polymorphisms and breast cancer risk*. 1999 Cancer Epidemiol. Biomarkers Prev. 8 843-854

3. Kwok P Y 2001 Annu. *Recovering frequencies of known haplotype blocks from single-nucleotide polymorphism allele frequencies*. Rev. Genomics Hum. Genet. 2 235-258

4. Tindall E A, Petersen D C, Woodbridge P, Schipany K and Hayes V M 2009 Hum. *Assessing high-resolution melt curve analysis for accurate detection of gene variants in complex DNA fragments.* Mutat. 30 876-883

5. van Grinsven B, Vanden Bon N, Strauven H, Grieten L, Murib M, Jiménez Monroy K L, Janssens S D, Haenen K, Schoning M J, Vermeeren V, Ameloot M, Michiels L, Thoelen R, De Ceuninck W and Wagner P. *Heat-Transfer Resistance at Solid_Liquid Interfaces: A Tool for the Detection of Single-Nucleotide Polymorphisms in DNA*.2012, ACS Nano 6 2712-2721

6. van Grinsven B, Vanden Bon N, Grieten L, Murib M, Janssens S D, Haenen K, Schneider E, Ingebrandt S, Schoning M J, Vermeeren V, Ameloot M, Michiels L, Thoelen R, De Ceuninck W and Wagner P. *Rapid assessment of the stability of DNA duplexes by impedimetric real-time monitoring of chemically induced denaturation* 2011 Lab Chip 11 1656-1663

7. Broeders J, Murib MS, Croux D, van Grinsven B, Wagner P, Thoelen R and Ceunink W. *Miniature detection system for DNA polymorphisms*, 2013

8. The Arduino Uno, http://arduino.cc/en/Main/ArduinoBoardUno

9. Öpik A, Menaker A, Reut J and Syritski V. *Molecularly imprinted polymers: a new approach to the preparation of functional materials*. Estonia, 2009

10. TravTigerEE, Wikimedia commons. 27 Jan 2013, PID_en_updated_feedback.svg. http://en.wikipedia.org/wiki/File:PID_en_updated_feedback.svg

11. Skogestad S. *Probably the best simple PID tuning rules in the world, journal of Process control*, 2001

12. Eersels K, van Grinsven B, Ethirajan A, Timmermans S, Monroy K L, Bogie J F J, Punniyakoti S, Vandenryt T, Hendriks J J A, Cleij T J, Daemen M J A P , Somers V, Ceuninck W D and Wagner P. *Selective identification of macrophages and cancer cells based on thermal transport through surface-imprinted polymer layers*. 2013

13. Ferencik, M. *Handbook of immunochemistry*. Chapman & Hall: London 1993

14. Schenkel-Brunner, H. *Human blood groups, chemical and biochemical basis of antigen specificity*. Springer: Heidelberg 2000

15. Mason, V.R. *J. Am. Med. Assoc.* 1922, 79, 1318-1320

16. Kolodgie, F.D.; Narula, J.; Burke, A.P.; Haider, N.; Farb, A.; Hiu-Lang, Y.; Smialek, J.; Virmani, R. *Am. J. Pathol.* 2000, 157, 1259-1268.

17. Blanc-Brude, O.P.; Teissier, E.; Castier, Y.; Lesèche, G.; Bijnens, A.P.; Daemen, M.; Staels, B.; Mallat, Z.; Tedgui, A. *Arterioscl. Throm. Vas.* 2007, 27, 901-907

18. Solatian P, Abbasi S H, Shabaninia F, *Simulation Study of Flow Control Based On PID ANFIS Controller for Non-Linear Process Plants, American Journal of Intelligent* Systems, 2165-8994, 2012; 2(5): 104-110

19. Hayden, O.; Mann, K.J.; Krassnig, S.; Dickert, F.L. *Angew. Chem. Int. Ed.* 2006, 45, 2626-2629

20. Qi, P., Wan, Y.; Zhang, D. *Biosens. Bioelectron.* 2013, 39, 282-288. 2626-2629

21. Mutharasan R, Magee W.E, Wheatley M.A., Lee Y.H. *Engineering Biotechnology*

22. Rivera, D.E., M. Morari, and S. Skogestad, *Internal Model Control 4. PID Controller Design*, Industrial Engineering and Chemical Process Design and Development, 25, p. 252, 1986

23. Putra Y H, S.T.,M.T. *Tuning methods of PID controller*, http://elib.unikom.ac.id/files/disk1/389/jbptunikompp-gdl-yeffryhand-19448-13-bab13.pdf

24. Ashley-Koch A, Yang Q, Olney RS. *Sickle hemoglobin (HbS) allele and sickle cell disease: a HuGE review.* Am J Epidemiol. 2000 May 1;151(9):839-45

25. *National Human Genome Research Institute,* http://www.genome.gov/glossary/)

26. Lazaridis G, *PID theory* , http://www.pcbheaven.com/wikipages/PID_Theory/ , 2011

27. Damos F S, Mendes R K, and Kubota L T. *Applications of QCM, EIS and SPR in the investigation of surfaces and interfaces for the development of (bio) sensors*. CP 6154, 13084-971 Campinas – SP

28. Rahman, A.R.A.; Lo, C.M.; Bhansali, S. *Sensor. Actuat. B-Chem.* 2006, 118, 115-120

29. Han, K.H.; Han, A.; Frazier, A.B. *Biosens. Bioelectron.* 2006, 21, 1907–1914

30. Chen, J.; Lib, J.; Sun, Y. *Lab. Chip.* 2012, 12, 1753-1767

31. O. A. Williams, M. Nesládek, M. Daenen, S. Michaelson, A. Hoffman, E. Osawa, K. Haenen and R.B. Jackman, Diam. Relat. Mater., 17 (2008), 1080-1088

Supplemental information

1. Constant temperature profile measurements

Constant temperature profiles have been obtained using PID parameters as follows (P = 0.40, I= 50, D = 0)

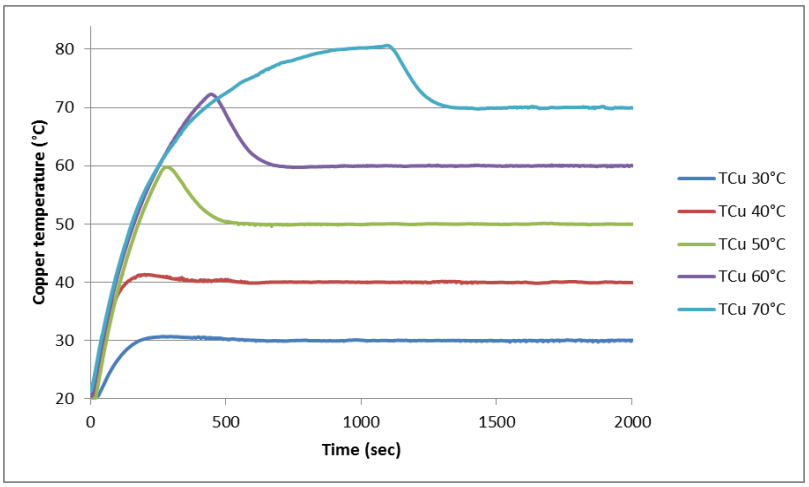

2. DNA denaturation detection (another successful measurement)

A denaturation experiment on a perfectly matched (ds) DNA sample:

- **Rth response VS TCu**

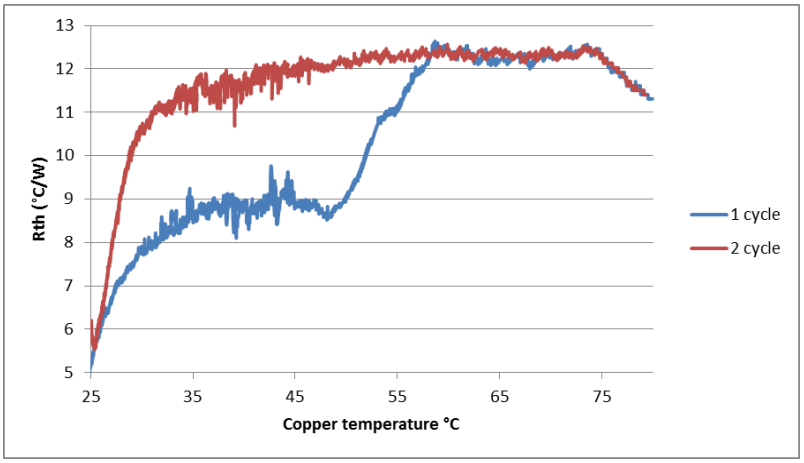

- **Applied ramping temperature profile**

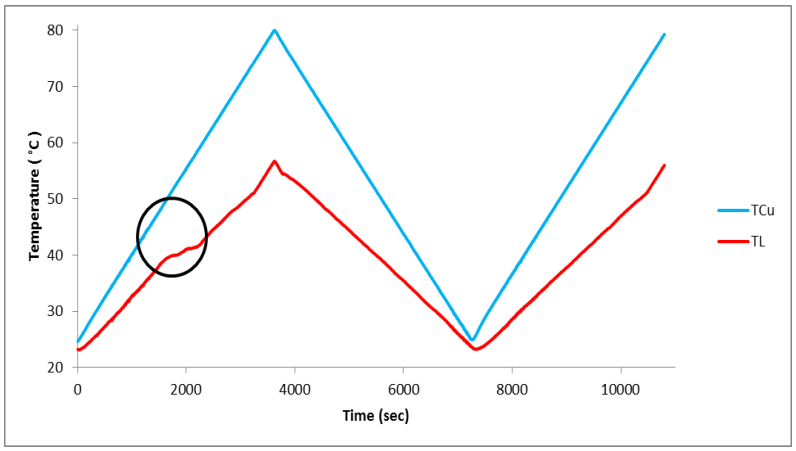

- **Temperature difference VS TCu** and **Voltage VS TCu**

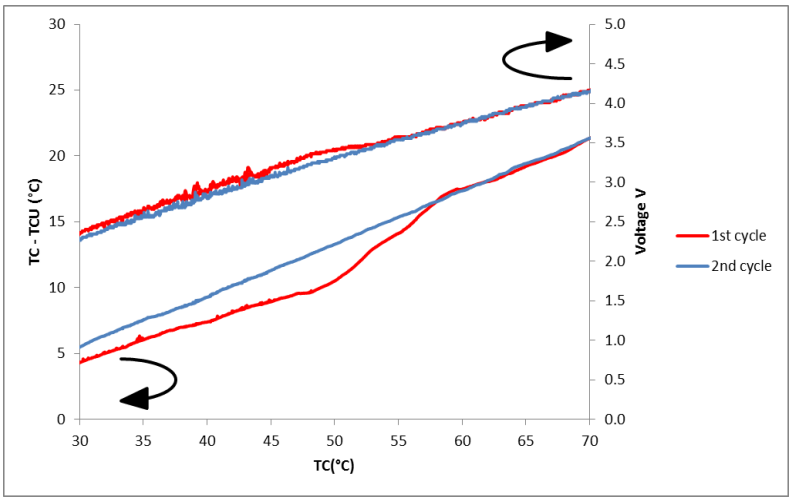

- **Power VS TCu**

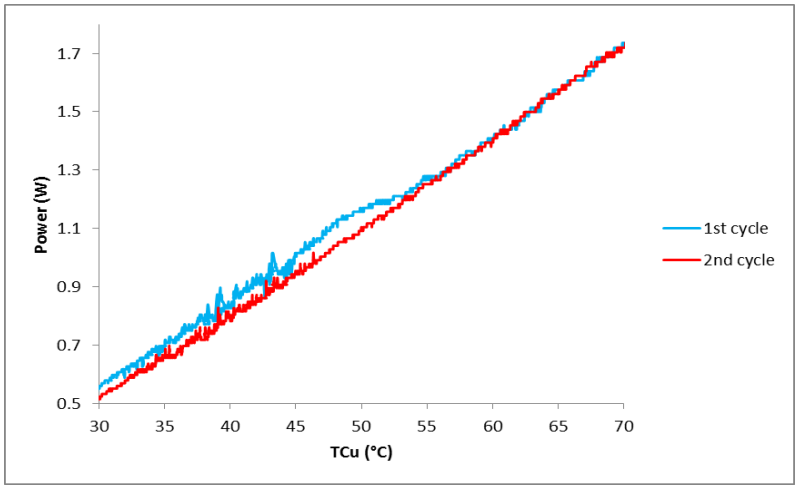

Auteursrechtelijke overeenkomst

Ik/wij verlenen het wereldwijde auteursrecht voor de ingediende eindverhandeling:
Optimization of thermal resistance system for biosensors

Richting: **master in de biomedische wetenschappen-bio-elektronica en nanotechnologie**
Jaar: **2013**

in alle mogelijke mediaformaten, - bestaande en in de toekomst te ontwikkelen - , aan de Universiteit Hasselt.

Niet tegenstaand deze toekenning van het auteursrecht aan de Universiteit Hasselt behoud ik als auteur het recht om de eindverhandeling, - in zijn geheel of gedeeltelijk -, vrij te reproduceren, (her)publiceren of distribueren zonder de toelating te moeten verkrijgen van de Universiteit Hasselt.

Ik bevestig dat de eindverhandeling mijn origineel werk is, en dat ik het recht heb om de rechten te verlenen die in deze overeenkomst worden beschreven. Ik verklaar tevens dat de eindverhandeling, naar mijn weten, het auteursrecht van anderen niet overtreedt.

Ik verklaar tevens dat ik voor het materiaal in de eindverhandeling dat beschermd wordt door het auteursrecht, de nodige toelatingen heb verkregen zodat ik deze ook aan de Universiteit Hasselt kan overdragen en dat dit duidelijk in de tekst en inhoud van de eindverhandeling werd genotificeerd.

Universiteit Hasselt zal mij als auteur(s) van de eindverhandeling identificeren en zal geen wijzigingen aanbrengen aan de eindverhandeling, uitgezonderd deze toegelaten door deze overeenkomst.

Voor akkoord,

Abu Zer, Ahmad

Datum: **10/06/2013**